Journal of Biomedical Optics

BiomedicalOptics.SPIEDigitalLibrary.org

Label-free high-throughput detection and quantification of circulating melanoma tumor cell clusters by linear-array-based photoacoustic tomography

Pengfei Hai
Yong Zhou
Ruiying Zhang
Jun Ma
Yang Li
Jin-Yu Shao
Lihong V. Wang

Pengfei Hai, Yong Zhou, Ruiying Zhang, Jun Ma, Yang Li, Jin-Yu Shao, Lihong V. Wang, "Label-free high-throughput detection and quantification of circulating melanoma tumor cell clusters by linear-array-based photoacoustic tomography," *J. Biomed. Opt.* **22**(4), 041004 (2016), doi: 10.1117/1.JBO.22.4.041004.

SPIE.

Label-free high-throughput detection and quantification of circulating melanoma tumor cell clusters by linear-array-based photoacoustic tomography

Pengfei Hai,† Yong Zhou,† Ruiying Zhang, Jun Ma, Yang Li, Jin-Yu Shao, and Lihong V. Wang*
Washington University in St. Louis, Department of Biomedical Engineering, Optical Imaging Laboratory, One Brookings Drive, St. Louis, Missouri 63130, United States

Abstract. Circulating tumor cell (CTC) clusters, arising from multicellular groupings in a primary tumor, greatly elevate the metastatic potential of cancer compared with single CTCs. High-throughput detection and quantification of CTC clusters are important for understanding the tumor metastatic process and improving cancer therapy. Here, we applied a linear-array-based photoacoustic tomography (LA-PAT) system and improved the image reconstruction for label-free high-throughput CTC cluster detection and quantification *in vivo*. The feasibility was first demonstrated by imaging CTC cluster *ex vivo*. The relationship between the contrast-to-noise ratios (CNRs) and the number of cells in melanoma tumor cell clusters was investigated and verified. Melanoma CTC clusters with a minimum of four cells could be detected, and the number of cells could be computed from the CNR. Finally, we demonstrated imaging of injected melanoma CTC clusters in rats *in vivo*. Similarly, the number of cells in the melanoma CTC clusters could be quantified. The data showed that larger CTC clusters had faster clearance rates in the bloodstream, which agreed with the literature. The results demonstrated the capability of LA-PAT to detect and quantify melanoma CTC clusters *in vivo* and showed its potential for tumor metastasis study and cancer therapy. [DOI: 10.1117/1.JBO.22.4.041004]

Keywords: photoacoustic tomography; cancer metastasis; circulating tumor cell clusters; cancer therapy.

Paper 160583SSR received Aug. 24, 2016; accepted for publication Oct. 19, 2016; published online Nov. 10, 2016.

1 Introduction

Metastasis, the spread of cancer cells from a primary site to distant organs leading to the growth of new tumors there, accounts for the majority of cancer deaths.[1] Blood-borne metastasis comprises multiple steps, including intravazation, survival in the blood circulation, extravazation, and secondary growth in the distant organs, in which the rare circulating tumor cells (CTCs) are the key determinants of metastatic propensity.[2] While most CTCs survive in the blood circulation in the form of single cells, CTC clusters also exist and elevate the metastatic potential by 23 to 50 folds.[3] Detection and quantification of CTC clusters will provide valuable insights into metastasis as well as cancer therapy. Because the presence of CTCs is positively correlated with metastatic propensity,[4] the detection and enumeration of rare CTCs will help to better evaluate the melanoma stage and predict metastatic potential during the diagnosis. In addition, tracking the concentration of CTCs in the circulatory system during treatment will likely be valuable indicators of both tumor responses to therapy and melanoma progression.

Taking advantage of tumor-specific physical and biological properties, such as sizes and surface biomarkers, multiple technologies have been developed to capture and isolate single CTCs and CTC clusters.[5–7] However, most of these existing technologies require blood to be drawn to isolate and capture CTCs *ex vivo*, reducing the effective CTC detection sensitivity. Optical imaging technologies, such as confocal microscopy, *in vivo* flow cytometry, and optical coherence tomography, have been applied to detect CTCs *in vivo*.[8–11] However, suffering from strong optical scattering in biological tissue, these techniques have shallow penetration, limiting them to imaging only small blood vessels, which results in low throughput for CTC detection.

By integrating optical excitation with acoustic detection, photoacoustic tomography (PAT) combines rich optical absorption contrasts with high ultrasonic spatial resolution at depths.[12] With 100% relative sensitivity to optical absorption, i.e., a given percentage change in the optical absorption yields the same percentage change in the photoacoustic signal, PAT achieves structural, functional, metabolic, and mechanical imaging of biological tissue.[13–17] Taking advantage of the strong optical absorption of melanin, photoacoustic techniques have been successfully used for imaging and sensing melanoma CTCs. Photoacoustic flowmetry successfully detected circulating melanoma cells in human blood.[18,19] Photoacoustic flow cytometry enables long-term monitoring of melanoma CTCs *in vivo*. However, these sensing techniques provide inadequate spatial resolution to further characterize melanoma CTCs.[20] The microscopic implementation of PAT, optical-resolution photoacoustic microscopy (OR-PAM), images single melanoma CTCs in the

*Address all correspondence to: Lihong V. Wang, E-mail: lhwang@wustl.edu

†These authors contributed equally to this work.

1083-3668/2016/$25.00 © 2016 SPIE

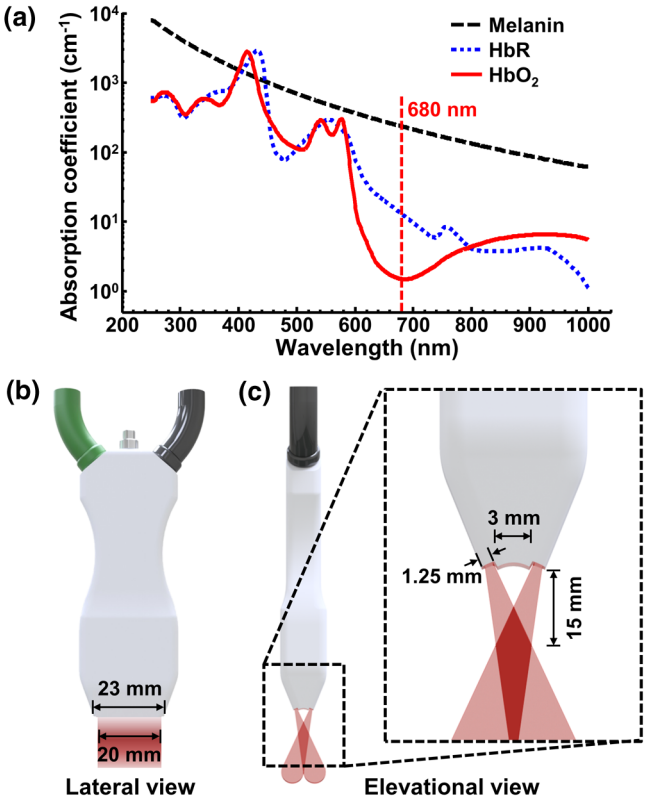

Fig. 1 Absorption spectra of melanin and hemoglobin, and the front and side views of the handheld probe for LA-PAT. (a) Absorption spectra of melanin and hemoglobin. An excitation wavelength of 680 nm was chosen for the optimal CNR. (b) Lateral view of the handheld probe. (c) Elevational view of the handheld probe with a zoomed-in view.

blood flows with high spatial-temporal resolution.[21] While providing valuable insights into CTCs on a single-cell level, OR-PAM suffers from low throughput.

Here, we apply a linear-array-based photoacoustic tomography (LA-PAT) system for label-free high-throughput melanoma CTC cluster detection and quantification *in vivo*. Exploiting the strong optical absorption of melanin in the melanoma tumor cells, LA-PAT can achieve label-free detection of melanoma CTC clusters *in vivo*. By analyzing the contrast-to-noise ratios (CNRs) of the photoacoustic signals, LA-PAT can quantify the number of cells in the CTC clusters and study their circulating kinetics in the bloodstream.

2 Materials and Methods

2.1 *Linear-Array-Based Photoacoustic Tomography System*

To image melanoma CTC clusters, we applied an LA-PAT system based on a handheld probe and improved the image reconstruction.[22] A tunable optical parametric oscillator laser (680 to 970 nm, 20-Hz pulse repetition rate) was used for illumination. An excitation wavelength of 680 nm was chosen to achieve the optimal contrast between melanoma tumor cells and blood [Fig. 1(a)]. The laser beam was coupled into a fiber optical bundle that bifurcated into two optical fiber bundles. Laser beams coming out of the two optical fiber bundle strips (20×1.25 mm^2) excited the object at an angle of incidence of 30 deg relative to the imaging plane [Figs. 1(b) and 1(c)]. During the experiments, the fluence on the tissue surface was about 10 mJ/cm^2, well within the 20 mJ/cm^2 safety limit set by the American National Standards Institute. The generated photoacoustic waves were detected by a linear array ultrasonic transducer (Visualsonics, Inc., LZ250, 21-MHz center frequency, 78% one-way bandwidth, 256 elements, 23×3 mm^2 array size). The spatial resolutions of the system were 119 μm in the lateral direction, 86 μm in the axial direction, and 1237 μm in the elevational direction.[23] Because there were only 64 channels in the data acquisition unit, four-to-one multiplexing was applied during image acquisition. For each laser pulse, the generated photoacoustic signals were captured sequentially by a quarter segment of the linear array (i.e., elements 1 to 64, 65 to 128, 129 to 192, and 193 to 256). Once the data were acquired from all four quarter segments, a two-dimensional photoacoustic image was reconstructed with the universal back-projection algorithm developed by our group.[24] The reconstructed photoacoustic images were displayed in an imaging station (Vevo LAZR, Visualsonics, Inc.). Determined by the 20-Hz laser repetition rate and the four-to-one multiplexing in image acquisition, the frame rate was 5 frames/s.

2.2 *Tumor Cell Culture and Cluster Preparation*

B16F10 melanoma tumor cells obtained from ATCC® were cultured in Dulbecco's modified Eagle's medium (Invitrogen) supplemented with 10% fetal bovine serum (Invitrogen) at 37°C in air with 5% CO_2. Upon reaching 80% confluence, cells growing in a monolayer were incubated with 0.25% trypsin-EDTA solution (Invitrogen) to generate floating cell clusters of various sizes. After adding serum-containing medium to neutralize trypsin, the floating cell clusters were handled in two ways. To mimic melanoma CTC clusters of various sizes, floating cell clusters totaling 1×10^6 cells were directly suspended in 1 mL of bovine blood for *ex vivo* experiments or in 1 mL of collected rat blood for tail vein injection. To generate melanoma cell clusters of a certain size for CNR analysis, instead of directly suspending the floating cell clusters in blood, the clusters were mechanically dissociated by pipetting to generate a single-cell suspension. The single cells were then suspended in a blood–agar mixture at a desired concentration and then cooled to become solid. The concentration was controlled so that within each resolution voxel of LA-PAT there was a certain number of melanoma cells, i.e., 5, 10, 20, 30, 40, or 50. The solid mixture was then mechanically dissociated into particles smaller than the resolution voxel of LA-PAT to generate cell clusters of a certain size. The particles were then suspended in 1 mL of bovine blood for CNR analysis.

2.3 *Phantom Preparation*

Silicone microtubes with 0.76 mm inner diameter (11-189-15C, Fisher Scientific) were perfused with bovine blood (905, Quad-Five) to mimic blood vessels. The microtubes were embedded 3 mm deep in tissue-mimicking gelatin phantoms. Optical scattering similar to that in biological tissue was achieved by adding 1% intralipid to the gelatin phantoms. Melanoma tumor cell clusters suspended in bovine blood were pumped through the microtubes with a syringe. A syringe pump (BSP-99M, Braintree Scientific) controlled the blood flow speed.

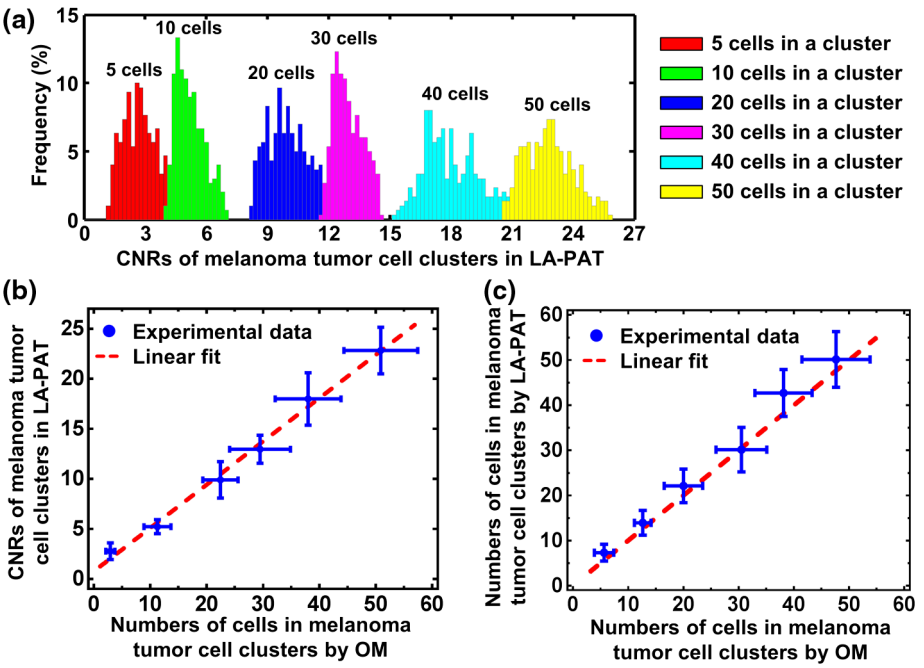

Fig. 2 CNR analysis of melanoma tumor cell clusters. (a) CNR distributions measured with LA-PAT for melanoma tumor cell clusters of different sizes. (b) Average CNRs in LA-PAT as a function of the numbers of cells in melanoma tumor cell clusters. (c) The numbers of cells in melanoma tumor cell clusters measured by LA-PAT agreed well with those measured by an OM.

2.4 *Experimental Animals and CTC Cluster Injection*

All experimental animal procedures were carried out in conformity with the laboratory animal protocol approved by the Animal Studies Committee at Washington University in St. Louis. Male nude rats (Hsd:RH-$Foxn1^{rnu}/Foxn1^{+}$, Harlan Co.; 12- to 13-weeks old; ~330 to 350 g body weight) were used for all *in vivo* experiments. Throughout the experiments, the rats were kept under anesthesia with 2% vaporized isoflurane. A homemade animal holder immobilized the rats during the experiments.

3 Results

3.1 *CNR Analysis of Melanoma Tumor Cell Clusters*

To detect and quantify CTC clusters, we first used LA-PAT to image melanoma tumor cell clusters of known sizes and analyzed their CNRs. Clusters with an average of 5, 10, 20, 30, 40, and 50 cells were suspended in blood and imaged by LA-PAT. The CNR for each cluster was calculated [Fig. 2(a)]. The average CNRs were plotted as a function of the number of cells in the clusters, as measured with an optical microscope (OM) (Eclipse TS100, Nikon) [Fig. 2(b)]. The experimental data were fitted to a linear function

$$\mathrm{CNR} = 0.46 \times N. \quad (1)$$

Here, N represents the number of cells in a melanoma tumor cell cluster. Based on a 6-dB CNR threshold, a minimum of four cells can be resolved although this minimum was not directly observed. To verify the relationship between the CNR and the number of cells in the clusters, another independent experiment was performed. Melanoma tumor cell clusters consisting of a uniform but unknown number of cells were equally divided into six groups. Three randomly chosen groups were suspended in blood and imaged by LA-PAT. The numbers of cells in the clusters were calculated based on the CNRs and the relationship above. The other three groups were examined with an OM to determine the numbers of cells in the clusters. The number of cells in the melanoma tumor cell clusters measured by LA-PAT and optical microscopy agreed well with each other [Fig. 2(c)], confirming the relationship between the numbers of cells in the clusters and the CNRs in LA-PAT.

3.2 *LA-PAT of CTC Clusters Ex Vivo*

We then demonstrated the ability of LA-PAT to detect and quantify CTC clusters *ex vivo*. A mixture of melanoma tumor cell clusters of various sizes was equally divided into six groups. Three randomly chosen groups were suspended in blood, pumped through microtubes to mimic flowing melanoma CTC clusters, and imaged by LA-PAT [Videos 1–3]. Each melanoma tumor cell cluster was captured by LA-PAT multiple times, and the average CNR was used to calculate the number of cells in the cluster. Based on the calculated number of cells in the clusters, the melanoma tumor cell clusters were divided into three categories: ≤10, 11 to 20, and ≥21. Typical photoacoustic images of the three categories are shown in Figs. 3(a)–3(c). The other three groups were measured with an OM to determine the numbers of cells in the clusters and were divided into the same three categories. The size distributions of the clusters measured by LA-PAT and optical microscopy agreed well with each other with a correlation coefficient of 0.96 [Fig. 3(d)], and the results further demonstrated the ability of LA-PAT to detect and quantify melanoma CTC clusters.

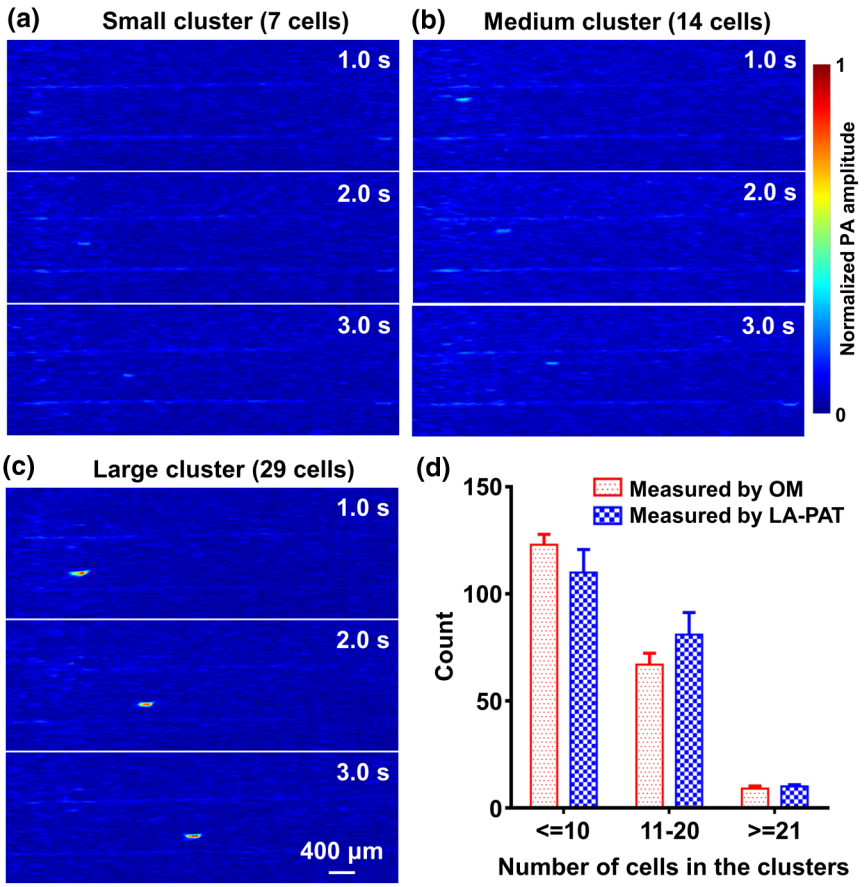

Fig. 3 LA-PAT of CTC clusters *ex vivo*. LA-PAT of a flowing melanoma tumor cell cluster with (a) 7 cells (Video 1), (b) 14 cells (Video 2), and (c) 29 cells (Video 3). The cell numbers are calculated based on the CNR curve in Fig. 2. (d) Distributions of the numbers of cells in melanoma tumor cell clusters, as measured by LA-PAT and OM (Video 1, MP4, 1.91 MB [URL: http://dx.doi.org/10.1117/1.JBO.22.4.041004.1]; Video 2, MP4, 2.01 MB [URL: http://dx.doi.org/10.1117/1.JBO.22.4.041004.2]; Video 3, MP4, 1.84 MB [URL: http://dx.doi.org/10.1117/1.JBO.22.4.041004.3]).

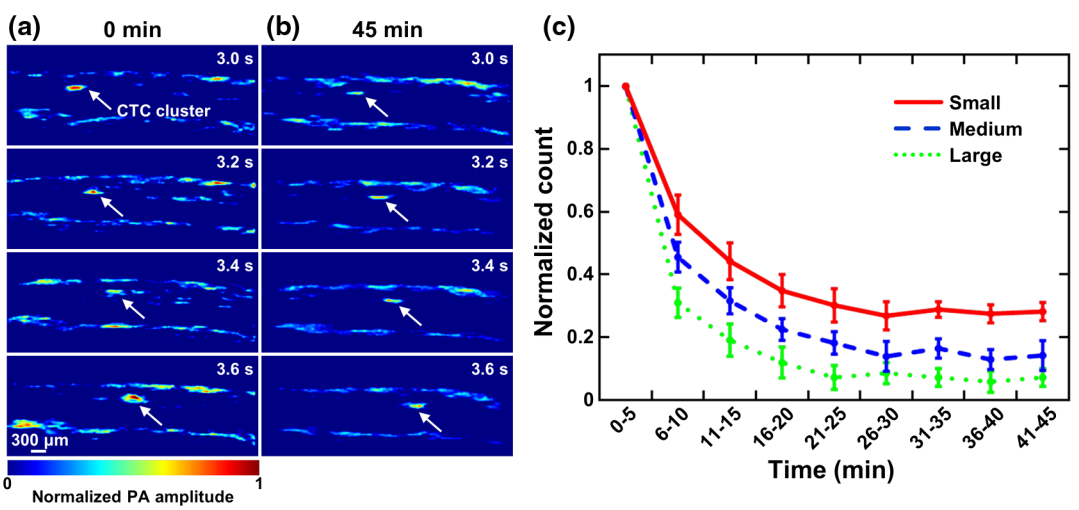

Fig. 4 LA-PAT of CTC clusters in rat tail veins *in vivo*. (a) LA-PAT of CTC clusters in a rat tail vein *in vivo* immediately after injection (Video 4). (b) LA-PAT of CTC clusters in the rat tail vein *in vivo* 45 min after injection (Video 5). (c) Clearance curves of small (≤10 cells), medium (11 to 20 cells), and large (≥21 cells) CTC clusters in rat bloodstreams (Video 4, MP4, 604 kB [URL: http://dx.doi.org/10.1117/1.JBO.22.4.041004.4]; Video 5, MP4, 613 kB [URL: http://dx.doi.org/10.1117/1.JBO.22.4.041004.5]).

3.3 *LA-PAT of CTC Clusters In Vivo*

To demonstrate the feasibility of LA-PAT *in vivo*, we imaged melanoma CTC clusters injected into rats. Melanoma tumor cell clusters suspended in 1 mL of rat blood at a concentration of 1×10^6 cells/mL were injected into the same rat from which the blood was collected a few minutes earlier. The rat tail vein was then monitored by LA-PAT for 45 min to study the circulation kinetics and the clearance rates of CTC clusters. CTC clusters were detected by LA-PAT immediately after injection and during circulating in the rat bloodstreams [Figs. 4(a) and 4(b) and Videos 4 and 5]. The numbers of cells in the CTC clusters were calculated based on the CNRs. The CTC clusters were categorized into three groups based on the calculated number of cells and the clearance curves of the three groups are shown in Fig. 4(c). Larger CTC clusters showed faster clearance rates from the bloodstream than smaller CTC clusters.

4 Discussion and Conclusions

Compared with single CTCs, CTC clusters are rarer, but have a higher metastatic potential. CTC clusters have a faster clearance rate, i.e., a shorter lifetime, in the bloodstream than single CTCs, making them even more difficult to detect. Here, we applied LA-PAT to detect and quantify melanoma CTC clusters in rat *in vivo*. Since the spatial resolutions of LA-PAT were not enough to resolve single melanoma tumor cells, the numbers of cells in the CTC clusters were quantified based on the CNRs. A linear relationship between the CNRs and the numbers of cells in the CTC clusters was found and verified. In *ex vivo* experiments, LA-PAT quantified the numbers of cells in the CTC clusters, and the results were validated by an OM. In experiments *in vivo*, LA-PAT detected and quantified melanoma CTC clusters immediately after injection, as well as when they were circulating in the rat bloodstreams. The results by LA-PAT also showed that larger CTC clusters have faster clearance rates.

The melanoma CTC detection sensitivity of LA-PAT is determined by the CNR. Because the noise is dominated by the fluctuating counts of red blood cells in each resolution voxel, the detection sensitivity is largely dependent on the spatial resolutions of LA-PAT. On one hand, to achieve single cell sensitivity in CTC detection, a higher frequency ultrasonic transducer could be used at the expense of penetration depth. On the other hand, to achieve deeper imaging, a lower frequency ultrasonic transducer can be employed, at the expense of CTC detection sensitivity. The CTC detection sensitivity can be further improved by performing spectral unmixing using multiwavelength illumination. To achieve multiwavelength imaging of flowing CTCs, a second laser with a different wavelength needs to be incorporated into the system.

It is worth pointing out that currently LA-PAT detects only CTCs originating from primary tumors in which cells express melanin. To detect CTCs originating from amelanotic melanoma tumors, other tumor-specific physiological properties, such as sizes and surface biomarkers, can be utilized. The quantification of CTC cluster sizes is indeed based on the assumption that the melanin content is relatively uniform in the tumor cells. This assumption often holds true for tumor cells originating from the same primary tumor. However, if there are several primary tumors, it may affect the accuracy of quantifying CTC cluster sizes.

LA-PAT has the potential to be a powerful tool for both preclinical tumor metastasis study and clinical cancer diagnosis and therapy. As a useful technique for researchers and scientists to better understand the relationship between CTCs and tumor metastasis, LA-PAT can employ ultrasonic transducers of different frequencies for target vessels at various depths and different animal models. Other physiological parameters, including vessel diameter and blood flow speed, can be measured concurrently for further understanding of CTC flow dynamics. LA-PAT can also be used by clinicians to monitor the changes of CTC concentrations in patients' circulatory systems and to evaluate the outcome of cancer therapy. To further improve LA-PAT for such clinical applications, an automatic CTC detection and counting algorithm should be developed.

Metastasis is a complex biological process that involves multiple steps and many parameters. Photoacoustic imaging, with the ability to quantify numerous parameters at multiple scales based on the same optical absorption contrast, can provide comprehensive information about tumor metastasis. OR-PAM can study CTCs on a single-cell level.[21] LA-PAT has been demonstrated to detect and quantify CTC clusters. In addition, photoacoustic imaging can measure other important biological parameters, including the oxygen saturation of hemoglobin, metabolic rate, and tumor stiffness,[25–27] all of which are closely related to metastasis.[28–30] With the capability to detect and quantify CTC clusters and the potential to provide multidimensional information on tumor metastasis, LA-PAT is a promising tool for both preclinical cancer metastasis study and clinical tumor therapy.

Acknowledgments

The authors appreciate Professor James Ballard's close reading of the paper and Eric Zhang's assistance in cell cluster preparation. This work was sponsored by the National Science Foundation Grant No. 1255930 and the National Institutes of Health (NIH) Grant Nos. R01 CA186567 (NIH Director's Transformative Research Award) and S10 RR026922 (VSI). L. V. Wang has a financial interest in Microphotoacoustics, Inc., which, however, did not support this work.

References

1. D. X. Nguyen, P. D. Bos, and J. Massagué, "Metastasis: from dissemination to organ-specific colonization," *Nat. Rev. Cancer* **9**(4), 274–284 (2009).
2. I. J. Fidler, "The pathogenesis of cancer metastasis: the 'seed and soil' hypothesis revisited," *Nat. Rev. Cancer* **3**(6), 453–458 (2003).
3. N. Aceto et al., "Circulating tumor cell clusters are oligoclonal precursors of breast cancer metastasis," *Cell* **158**(5), 1110–1122 (2014).
4. M. Cristofanilli et al., "Circulating tumor cells, disease progression, and survival in metastatic breast cancer," *N. Engl. J. Med.* **351**(8), 781–791 (2004).
5. M. Yu et al., "Circulating tumor cells: approaches to isolation and characterization," *J. Cell Biol.* **192**(3), 373–382 (2011).
6. S. Nagrath et al., "Isolation of rare circulating tumour cells in cancer patients by microchip technology," *Nature* **450**(7173), 1235–1239 (2007).
7. A. F. Sarioglu et al., "A microfluidic device for label-free, physical capture of circulating tumor cell clusters," *Nat. Methods* **12**(7), 685–691 (2015).
8. E. Sahai, "Illuminating the metastatic process," *Nat. Rev. Cancer* **7**(10), 737–749 (2007).
9. H. Seo et al., "*In vivo* quantitation of injected circulating tumor cells from great saphenous vein based on video-rate confocal microscopy," *Biomed. Opt. Express* **6**(6), 2158–2167 (2015).
10. I. Georgakoudi et al., "*In vivo* flow cytometry: a new method for enumerating circulating cancer cells," *Cancer Res.* **64**(15), 5044–5047 (2004).
11. S. M. Azarin et al., "*In vivo* capture and label-free detection of early metastatic cells," *Nat. Commun.* **6**, 8094 (2015).

12. L. V. Wang and S. Hu, "Photoacoustic tomography: *in vivo* imaging from organelles to organs," *Science* **335**(6075), 1458–1462 (2012).
13. P. Hai et al., "Near-infrared optical-resolution photoacoustic microscopy," *Opt. Lett.* **39**(17), 5192–5195 (2014).
14. J. Ma et al., "Grueneisen relaxation photoacoustic microscopy *in vivo*," *J. Biomed. Opt.* **21**(6), 066005 (2016).
15. X. Wang et al., "Noninvasive laser-induced photoacoustic tomography for structural and functional *in vivo* imaging of the brain," *Nat. Biotechnol.* **21**(7), 803–806 (2003).
16. J. Yao et al., "Label-free oxygen-metabolic photoacoustic microscopy *in vivo*," *J. Biomed. Opt.* **16**(7), 076003 (2011).
17. P. Hai et al., "Photoacoustic elastography," *Opt. Lett.* **41**(4), 725–728 (2016).
18. R. M. Weight et al., "Photoacoustic detection of metastatic melanoma cells in the human circulatory system," *Opt. Lett.* **31**(20), 2998–3000 (2006).
19. R. M. Weight, P. S. Dale, and J. A. Viator, "Detection of circulating melanoma cells in human blood using photoacoustic flowmetry," in *Annual Int. Conf. of the IEEE Engineering in Medicine and Biology Society (EMBC '09)*, pp. 106–109 (2009).
20. E. I. Galanzha and V. P. Zharov, "Photoacoustic flow cytometry," *Methods* **57**(3), 280–296 (2012).
21. L. Wang et al., "Photoacoustic imaging of single circulating melanoma cells *in vivo*," *Proc. SPIE* **9323**, 93230A (2015).
22. A. Needles et al., "Development and initial application of a fully integrated photoacoustic micro-ultrasound system," *IEEE Trans. Ultrason. Ferroelectr. Freq. Control* **60**(5), 888–897 (2013).
23. P. Hai et al., "Photoacoustic tomography of vascular compliance in humans," *J. Biomed. Opt.* **20**(12), 126008 (2015).
24. M. Xu and L. V. Wang, "Universal back-projection algorithm for photoacoustic computed tomography," *Phys. Rev. E* **71**(1), 016706 (2005).
25. H. F. Zhang et al., "Functional photoacoustic microscopy for high-resolution and noninvasive *in vivo* imaging," *Nat. Biotechnol.* **24**(7), 848–851 (2006).
26. J. Yao et al., "Noninvasive photoacoustic computed tomography of mouse brain metabolism *in vivo*," *NeuroImage* **64**(1), 257–266 (2013).
27. P. Hai et al., "Quantitative photoacoustic elastography in humans," *J. Biomed. Opt.* **21**(6), 066011 (2016).
28. G. P. Luke and S. Y. Emelianov, "Label-free detection of lymph node metastases with US-guided functional photoacoustic imaging," *Radiology* **277**(2), 435–442 (2015).
29. Y. Fong et al., "Breast-cancer-secreted miR-122 reprograms glucose metabolism in premetastatic niche to promote metastasis," *Nat. Cell Biol.* **17**(2), 183–194 (2015).
30. J. Fenner et al., "Macroscopic stiffness of breast tumors predicts metastasis," *Sci. Rep.* **4**, 5512 (2014).

Pengfei Hai is currently a PhD candidate in biomedical engineering at Washington University in St. Louis, under the supervision of Prof. Lihong V. Wang. He received his BS degree in biomedical engineering from Shanghai Jiao Tong University in 2012. His research interests include the technical development and biomedical applications of photoacoustic imaging.

Yong Zhou is currently a graduate student in biomedical engineering at Washington University in St. Louis, under the supervision of Dr. Lihong V. Wang, Gene K. Beare Distinguished Professor. His research focuses on the development of photoacoustic imaging systems.

Ruiying Zhang received her BS degree in optical information science and technology from Wuhan University in Hubei, China. She is currently a PhD student in the Department of Biomedical Engineering at Washington University in St. Louis. Her research interests include optical and photoacoustic/ultrasound imaging with biomedical applications.

Jun Ma received his BSc degree from Huazhong University of Science and Technology and a PhD from the Hong Kong Polytechnic University. Currently, he is working as a postdoctoral research associate at the Biomedical Engineering Department, Washington University in St. Louis. His research interests include optical acoustic and ultrasonic transducer and photoacoustic imaging and its biomedical applications.

Yang Li received his degree of BS *summa cum laude* in biomedical engineering from the State University of New York at Buffalo in 2013. Then he joined the Optical Imaging Laboratory at Washington University in St. Louis to pursue the degree of PhD in the same field. He is currently working on high-speed, high-throughput detection methods for photoacoustic imaging.

Jin-Yu Shao: Biography is not available.

Lihong V. Wang is a Gene K. Beare Distinguished Professor at Washington University, has published 437 journal articles (h-index = 108, citations > 47,000) and delivered 433 keynote/plenary/invited talks. His laboratory published the first functional photoacoustic CT and three-dimensional photoacoustic microscopy. He received the Goodman Award for his Biomedical Optics textbook, NIH Director's Pioneer Award, OSA Mees Medal, IEEE Technical Achievement and Biomedical Engineering Awards, SPIE Britton Chance Biomedical Optics Award, and an honorary doctorate from Lund University, Sweden.